



HAL
open science

Hyperfine interactions in homonuclear diatomic molecules and u-g perturbations. II. Experiments on I2

J. P. Pique, F. Hartmann, S. Churassy, R. Bacis

► **To cite this version:**

J. P. Pique, F. Hartmann, S. Churassy, R. Bacis. Hyperfine interactions in homonuclear diatomic molecules and u-g perturbations. II. Experiments on I2. *Journal de Physique*, 1986, 47 (11), pp.1917-1929. 10.1051/jphys:0198600470110191700 . jpa-00210388

HAL Id: jpa-00210388

<https://hal.science/jpa-00210388>

Submitted on 4 Feb 2008

HAL is a multi-disciplinary open access archive for the deposit and dissemination of scientific research documents, whether they are published or not. The documents may come from teaching and research institutions in France or abroad, or from public or private research centers.

L'archive ouverte pluridisciplinaire **HAL**, est destinée au dépôt et à la diffusion de documents scientifiques de niveau recherche, publiés ou non, émanant des établissements d'enseignement et de recherche français ou étrangers, des laboratoires publics ou privés.

Classification
 Physics Abstracts
 31.30 — 35.20S — 33.20K

Hyperfine interactions in homonuclear diatomic molecules and u-g perturbations. II. Experiments on I₂

J. P. Pique (*), F. Hartmann (*), S. Churassy (**), and R. Bacis (**)

(*) Université Scientifique, Technologique et Médicale de Grenoble, Laboratoire de Spectrométrie Physique, B.P. 87, 38402 Saint Martin d'Hères Cedex, France

(**) Université Claude Bernard, Lyon I, Laboratoire de Spectrométrie Ionique et Moléculaire, 43, bd du 11-Novembre-1918, 69622 Villeurbanne Cedex, France

(Reçu le 27 septembre 1985, révisé le 27 juin 1986, accepté le 28 juillet 1986)

Résumé. — L'état B 0_u⁺ de l'iode est étudié près de sa limite de dissociation par une technique sub-Doppler haute résolution. L'enregistrement de plus de 10 000 raies hyperfines permet une étude systématique de la structure hyperfine. Toutes les observations peuvent être interprétées à partir du calcul des interactions hyperfines dues aux autres états électroniques ayant la même limite de dissociation. Trois situations différentes sont rencontrées : les perturbations faibles traitées dans la théorie de Broyer, Vigué et Lehmann de l'approximation du second ordre, les structures superhyperfines observées dans plusieurs têtes de bande et le cas des perturbations fortes ($v' = 76, 77$ et 78). Cette dernière situation a demandé l'utilisation de la matrice complète d'interaction de l'état B 0_u⁺ avec un état 1 g, conduisant à la première mise en évidence d'une brisure de symétrie u-g dans une molécule diatomique homonucléaire.

Abstract. — The iodine B 0_u⁺ state is studied near its dissociation limit using sub-Doppler high resolution techniques. The recording of more than 10 000 hyperfine lines allows a systematic analysis of the hyperfine structure. All the observed features can be accounted for by the calculation of the interactions of the B state with the other electronic states sharing the same dissociation limit. Three different situations are encountered : weak perturbation situations treated in the second-order approximation of the Broyer, Vigué, Lehmann theory, superhyperfine structures observed in several band heads, and strong perturbation cases (vibrational levels $v' = 76, 77$ and 78). This last situation has required the utilization of the full exact interaction matrix of B 0_u⁺ with a 1 g state, leading to the first direct evidence of a u-g symmetry breaking in a homonuclear diatomic molecule.

1. Introduction.

The second dissociation limit ${}^2P_{1/2} + {}^2P_{3/2}$ of the ${}^{127}\text{I}_2$ molecule is the origin of 10 molecular electronic states [1]. Since atomic iodine has a nuclear spin $\frac{5}{2}$, all these molecular states have a hyperfine structure. For example one of them, the B ${}^3\Pi_0^+$ state has a hyperfine structure of the order of 1 GHz. For low B state vibrational levels, this hyperfine structure (h.f.s.) is weak compared to rotational separations, and all the possible perturbations can be accurately described by a second-order perturbation Hamiltonian [2a, b, c]. But for increasing internuclear distance, the rotational and even electronic separations decrease and become comparable to the hyperfine structure, and strong hyperfine perturbations are to be expected between rovibrational levels of different electronic states lying close to the dissociation limit.

Except the B state, which is known in its rovibrational structure up to $v' = 80$ [3], all the other electronic states are only sketchily known experimentally, so that the study of strong hyperfine perturbations in the B state requires a systematic investigation of the near-dissociation limit.

We have undertaken an extensive high resolution analysis of the hyperfine structure of rovibrational B state levels from 28 cm^{-1} to 0.5 cm^{-1} below the ${}^2P_{1/2} + {}^2P_{3/2}$ dissociation limit, that is from $v' = 71$ to $v' = 82$. In a first paper (part I) we have reported the theoretical framework of hyperfine interactions in homonuclear diatomic molecules. This second paper presents the experimental checks of these theoretical predictions through the example of the ${}^{127}\text{I}_2$ B state. Section 2 describes the experimental technique and the data acquisition system for the more than 10 000 hyperfine lines recorded. Section 3 presents a systematic survey of the observed spectra and their interpretation with a second-order pertur-

bation approximation or a direct interaction matrix, depending on the importance of the perturbation effects.

2. Experimental.

The observation of hyperfine structure in the iodine B state requires sub-Doppler resolution. Saturated absorption spectroscopy and molecular beam are the two main techniques allowing sub-Doppler spectroscopy, with the resulting resolution limited only by the laser spectral width. For our study in the dissociation limit region, the $X 0_g^+ - B 0_u^+$ transition moment becomes weak, and it would be difficult to saturate the concerned transitions. Moreover, in the vicinity of the dissociation limit only the first rotational levels are bound, and they are to be excited from the first J'' levels of the ground state. In a cell, the iodine pressure of a few ten millitorrs gives a weak population of these first J'' levels. As a result, the saturated absorption technique cannot be used for our purpose, and we have developed an iodine supersonic molecular beam.

In this technique, high molecular density and significant rotational cooling can be easily achieved, and these two advantages greatly favor the observation of weakly bound excited B state levels. The experimental set-up has been described previously [4]. For this experiment some improvements have been made (Fig. 1). The expansion chamber and the interaction chamber have large stainless steel liquid nitrogen traps which provide an efficient cryogenic pumping. The pressure in the two chambers is about 10^{-6} torr. At a generating temperature in the iodine oven of about 60°C , the molecular beam can be operated for 4 to 5 hours before clogging of the first nitrogen trap occurs. The interaction chamber can be isolated from the expansion chamber by a gate valve. This allows the opening and cleaning of the expansion chamber with the second chamber still under vacuum, so that the molecular beam can be reset within one hour. The operating conditions are similar to those described previously [4], except for the collimating ratio which here is $1/500$ in order to reduce the Doppler width below 1 MHz.

The molecular beam is crossed at right angle by the laser beam of a single mode ring dye laser (Coherent Radiation CR 699-21). Coumarin 102 dye pumped by a Kr^+ laser gives an output power of about 100 mW, tunable in the region 490 to 510 nm. In this frequency range, the laser performance is very sensitive to optical surface pollution, and the ring laser must be placed inside a box with a dust-preventing weak nitrogen gas flow in order to maintain a sufficient output power over a few hours.

The experimental data consist of two signals simultaneously recorded: the beam fluorescence monitored by a photomultiplier (EMI 9658A) working in the photon counting mode and the frequency measurements given by a lambdameter [5].

When special care is taken for the improvement of the detection efficiency, such as light baffles and

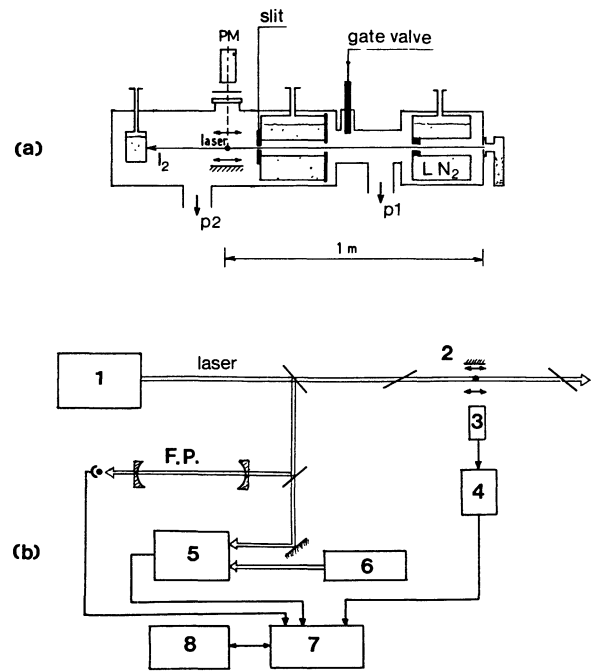


Fig. 1. — Experimental set-up. (a): The supersonic molecular beam apparatus. The expansion chamber (pumped by P_1) can be isolated from the interaction chamber (pumped by P_2) by a gate valve. The slit and hole of the I_2 reservoir define the molecular beam of iodine (in the figure plane). The beam is crossed at right angle by the laser beam. The fluorescence light is directed to a photomultiplier (EMI 9658 A) through a colour filter. (b): Complete experimental scheme. 1: Single mode tunable dye laser (Coherent Radiation model 699-21). 2: Molecular beam. 3: Photomultiplier. 4: Photon counter. 5: Lambdameter. 6: Wavelength reference given by a I_2 -stabilized He-Ne laser. 7: Microcomputer recording the fluorescence signal from 4, the laser wavelength from 5 and the reference fringes given by a confocal Fabry-Perot (F. P.) of 81 MHz F.S.R. 8: Computer.

diaphragms in the laser path reducing the laser stray light, photomultiplier cooling at -10°C by Peltier effect and pulse discrimination from the electronic noise in the photon counting chain, the overall background can be reduced to less than 100 counts per second. The resulting signal to background ratio is then more than 500 for the strongest observed hyperfine transitions.

The frequency scale as well as the identification of a rotational line are given by a lambdameter which compares the laser wavelength to a reference iodine-stabilized He-Ne laser. For an accuracy of 10^{-4} Å (12 MHz) in the wavelength determination each measurement needs 3 s. Since under typical conditions the laser is scanned at a rate of 3 MHz per second, each measurement is a mean value for a scan of about 10 MHz.

Both digital signals of photon counter and lambda-diameter are acquired by a microcomputer. The fringes of a confocal Fabry-Perot are also recorded as a monitor of the laser scan. For a sampling rate of 5 measurements per MHz, which is compatible with the 1 MHz laser spectral width, the microcomputer disc can store the data of a 4 GHz run, sufficiently larger than the typical h.f.s. pattern of about 1 GHz. The use of a microcomputer allows the recording of a large number of h.f.s. lines and also the complete direct numerical data processing. The computer calculates the frequency scale from a least squares fit to the lambda-diameter measurements. The time evolution of the laser frequency is quasi-linear but, in order to have a relative precision of the order of 1 MHz, a fit to a third-order polynomial was performed to determine the frequency scale. The root mean square scatter of the lambda-diameter points with respect to this scale is about 20 MHz. Once the frequency scale is defined, a subroutine determines the position and intensity of each hyperfine transition. The whole process for a 4 GHz scan takes less than half an hour. Reproducibility and relative precision of the measured lines are of the order of 1 MHz. Figure 2 gives an example of the recorded spectra close to the 72-0 band head. Also displayed are the transmission fringes of a confocal Fabry-Perot of 81 MHz free spectral range. The well known sensitivity of a Fabry-Perot to thermal drifts prevents its use as a frequency scale accurate to 1 MHz; it was used here, as already stated, as a monitor of the laser scan, detecting any scan speed variations or mode hops.

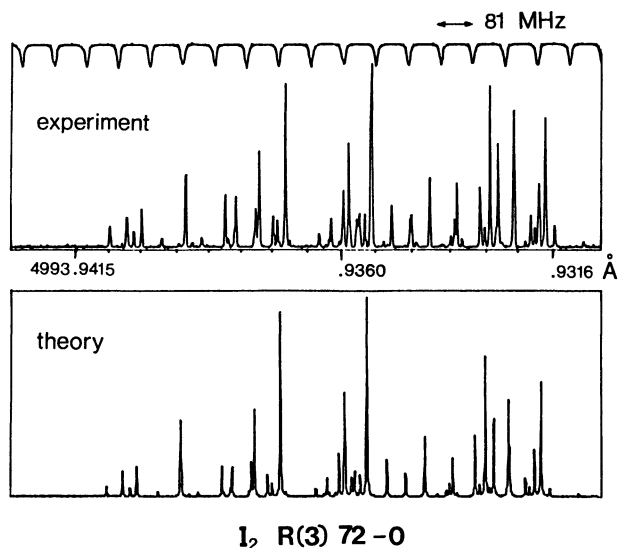


Fig. 2. — Hyperfine structure of the R (3) 72-0 B ← X transition. The wavelength scale is given by the lambda-diameter. It is calculated from a third order polynomial fit to the lambda-diameter measurements obtained during the laser frequency scanning. The relative precision is of the order of 1 MHz. The upper trace is the transmission fringes of a confocal Fabry-Perot of 81 MHz F.S.R., used as a monitor of the laser scan. The R.M.S. deviation in the fit to the recorded spectrum is 2.5 MHz.

3. Hyperfine structure near the B state dissociation limit.

This work concerns the last 30 cm^{-1} below the $^2P_{1/2} + ^2P_{3/2}$ dissociation limit. All the vibrational levels from $v' = 71$ to the last observable level $v' = 83$ have been studied in a systematic way, which represents more than 10 000 recorded hyperfine transitions. As hyperfine perturbations of the B state vary from level to level, the related h.f.s. patterns exhibit large differences. However, they can be classified in three main kinds. In the increasing order of perturbation, we have first the weak interactions case for which a second-order perturbation Hamiltonian gives an accurate representation, and the hyperfine spectra are very similar to those of lower B state vibrational levels. The second case is encountered in some band heads, in which the rotational spacings are of the same order of magnitude as the hyperfine interactions, so that the hyperfine Hamiltonian must include several neighbouring rotational levels, leading to the superhyperfine structures [6a, b]. In the third case, the B state perturbation by other electronic states becomes important, especially when resonances occur. The hyperfine structure is then deeply modified, such as in the perturbation by a 1 g state, leading to the u-g mixing.

3.1 WEAK HYPERFINE PERTURBATIONS. — In this systematic B-state hyperfine study, numerous rovibrational levels exhibit hyperfine structures which have a pattern reminiscent of those previously observed for lower vibrational levels. These represent the case of weak hyperfine perturbations, for which the model Hamiltonian and the related theoretical analysis are well established [2]. We present here this case in two parts. The first gives the experimental results for all the observed levels and the second discusses all the possible contributions from the different perturbing electronic states and compares them to the observed perturbations.

3.1.1 Experimental analysis. — For our experimental accuracy of the order of 1 MHz, the hyperfine interactions can be described from a Hamiltonian limited to tensorial terms of rank 1 and 2 (magnetic dipolar and electric quadrupolar interactions) as developed in part I. But as long as the hyperfine perturbations are weak, from the hyperfine gyroscopic Hamiltonian H_{hfg} ((4) in part I) effective parameters can be defined in second-order approximation [2]. These effective parameters are termed $eQq' =$ quadrupolar, $C' =$ spin-rotation, $d' =$ tensorial spin-spin and $\delta' =$ scalar spin-spin interactions. They quantitatively describe the hyperfine structure of the rovibrational levels analysed until this work.

The observed B-X hyperfine spectra were computer fitted using the matrix elements calculated in this second-order approximation, the hyperfine parameters of the $X \ ^1\Sigma_g^+$ ground state being fixed at their known values [7]: $eQq'' = -2\ 452.58 \text{ MHz}$, $C'' = 3 \text{ kHz}$, $d'' = \delta'' = 0$.

This method enables us to fit the h.f.s. of rovibrational levels in three regions : i) $71 \leq v' \leq 75$, ii) $v' = 76$ for $J' < 15$ and iii) $79 \leq v' \leq 82$. The results are given in figures 3 and 4. In these figures, the dots and crosses represent the experimental values, while the full lines indicate the theoretical predictions which will be discussed later. In this work, each vibrational level is studied through several rotational lines. Figures 3 and 4 show that, although for $v' \leq 75$ and $v' \geq 79$ the obtained parameters are not J' dependent, for $v' = 76$ all the effective parameters except C' exhibit strong variations with J' . This behaviour denotes the beginning of strong hyperfine perturbations in the $v' = 76$ levels, this fact being supported by the study of $v' = 77$ and 78 , for which no effective parameters can be defined within the second-order treatment. Apart from these limiting cases, the effective parameters have a monotonic evolution with the vibrational quantum number v' . Such a smooth variation calls for a quantitative interpretation with the possible perturbing electronic states, and this encourages us to undertake the full theoretical analysis of the origin of the h.f.s. second order parameters.

3.1.2 The B state perturbations in the second order approximation. — The effective parameters eQq' , C' , d' and δ' can describe very precisely the hyperfine structure [7]. They have been analysed in detail in reference [8]. When all the perturbing electronic states Ω are taken into account, the effective B 0_u^+ state parameters can be expressed as :

$$\begin{aligned}
 C' &= C'_D + \frac{\beta g I_a}{\sqrt{2}} \sum_{1u} \langle \bar{V}^0 \rangle \langle \bar{V}^1 \rangle \sum_v \frac{\langle v|v' \rangle^2}{\Delta E_{vv'}^{J'}} \\
 \delta' &= \frac{2}{3} \left(\frac{\beta g I_a}{(\sqrt{2})^\epsilon} \right)^2 \sum_{\Omega} \chi_i(\Omega) \langle \bar{V}^1 \rangle^2 \sum_v \frac{\langle v|v' \rangle^2}{\Delta E_{vv'}^{J'}} \\
 d' &= d'_D + \frac{1}{2} \left(\frac{\beta g I_a}{(\sqrt{2})^\epsilon} \right)^2 \sum_{\Omega} (3\Omega^2 - 2) \chi_i(\Omega) \langle \bar{V}^1 \rangle^2 \sum_v \frac{\langle v|v' \rangle^2}{\Delta E_{vv'}^{J'}} \\
 eQq' &= eQq'_0 + \frac{eQ}{2\sqrt{3}} \sum_{1u} \langle \bar{V}^0 \rangle \langle \bar{V}^2 \rangle \sum_v \frac{\langle v|v' \rangle^2}{\Delta E_{vv'}^{J'}} \\
 &+ \left[\sum_{k,k'=1,2} (-1)^{2I_a} \frac{2C_k C_{k'}}{(\sqrt{2})^\epsilon} \begin{Bmatrix} I_a & 2 & I_a \\ k & I_a & k' \end{Bmatrix} \times \sum_{\Omega} (-1)^{\Omega} \begin{pmatrix} k & k' & 2 \\ \Delta\Omega & -\Delta\Omega & 0 \end{pmatrix} \langle \bar{V}^k \rangle \langle \bar{V}^{k'} \rangle \times \sum_v \frac{\langle v|v' \rangle^2}{\Delta E_{vv'}^{J'}} \right]. \quad (2)
 \end{aligned}$$

The quantities C'_D , d'_D and eQq'_0 refer to the first-order approximation, all the other quantities being defined in the theoretical analysis (part I) or in reference [9]. It has been shown that C'_D and d'_D are negligible [2a, 8a]. From the atomic parameters (see part I) it is easy to calculate $eQq'_0 = -573$ MHz. The sum over v is for all the vibrational quantum numbers v of a given perturbing Ω state. The denominator $\Delta E_{vv'}^{J'}$ is the energy separation between the perturbing level and the considered B state level : $\Delta E_{vv'}^{J'} = E_{\Omega v'} - E_{0_u^+ v' J'}$.

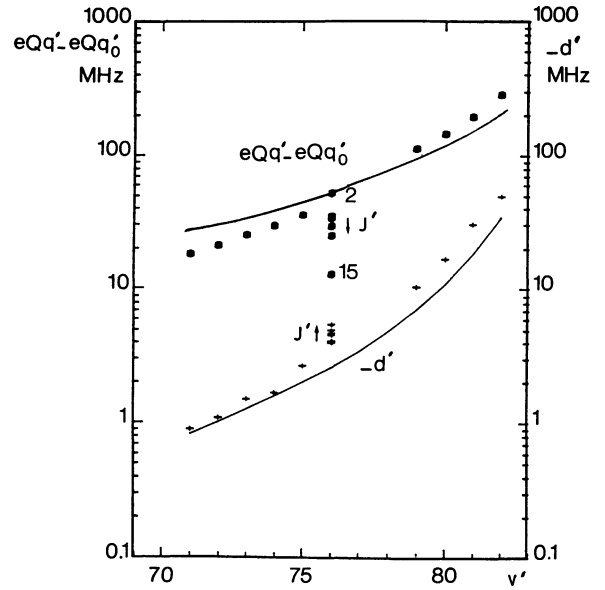


Fig. 3. — Effective parameter variations with the B state vibrational levels v' : electric quadrupolar eQq ($eQq'_0 = -573$ MHz) and tensorial spin-spin d' terms. The full lines represent the theoretical predictions at $J' = 0$ (Sect. 3.1.2). For the $v' = 76$ level the analysis shows a J' -dependence of the hyperfine parameters. The arrows indicate the increasing order in J' , from $J' = 2$ to 15. For every v' level except $v' = 76$, the experimental points correspond to the average of the measurements at various J' .

For brevity the relations (2) will be written :

$$C' = C'_D + \sum_{i_u i_g} C'_{0i}(\Omega)$$

$$\delta' = \sum_{\Omega} \delta'_{11}(\Omega)$$

$$d' = d'_D + \sum_{\Omega} d'_{11}(\Omega)$$

$$\text{and } eQq' = eQq'_0 + eQq'_{02} + \sum_{kk'} \sum_{\Omega} eQq'_{kk'}(\Omega),$$

the indexes referring to the reduced matrix elements $\langle \bar{V}^i \rangle$ involved in (2).

From the known $\langle \bar{V}^i \rangle$ values (paper I), a detailed analysis of relations (2) shows that the eQq' expression can be greatly simplified. The only significant contributions to eQq' apart from the eQq'_0 term come from $eQq'_{11}(\Omega)$ and $eQ(q'_{12}(\Omega) + q'_{21}(\Omega))$, that are :

$$eQq'_{11}(\Omega) = \chi_i(\Omega) (-1)^{\Omega+1} \delta'_{11}(\Omega)$$

$$eQ(q'_{12}(\Omega) + q'_{21}(\Omega)) = \chi_i(\Omega) \frac{3\Omega\sqrt{4-\Omega^2}}{2\sqrt{2}(3\Omega^2-2)} \frac{\frac{1}{2}eQ\langle \bar{V}^2 \rangle}{\beta g l_a \langle \bar{V}^1 \rangle} \delta'_{11}(\Omega) \quad (3)$$

$$\text{and moreover : } d'_{11}(\Omega) = \frac{3\Omega^2-2}{2} \delta'_{11}(\Omega),$$

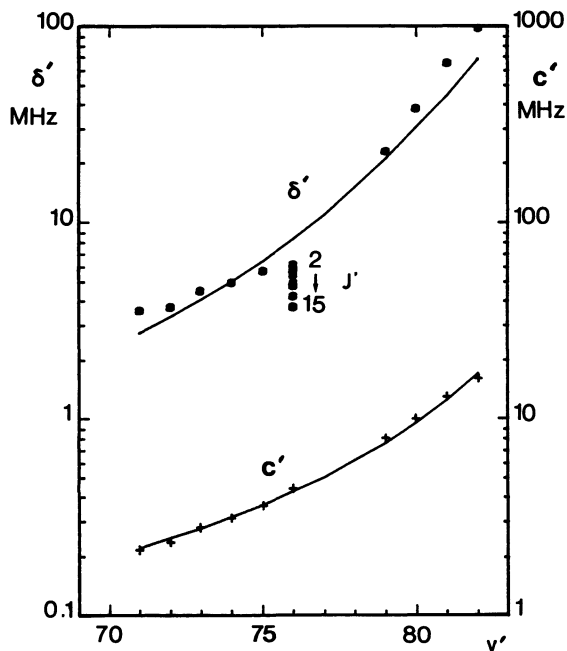


Fig. 4. — Effective parameter variations with the B state vibrational levels v' : scalar spin-spin δ' and spin-rotation C' terms. δ' has a strong J' -dependence in the $v' = 76$ level but C' is constant in this level. For full lines and experimental points see caption of figure 3.

so that the contribution to d' and eQq' of each Ω perturbing state needs only the calculation of $\delta'_{11}(\Omega)$.

Through these approximations, it can be shown that the perturbations by the $\Omega = 2$ states are negligible. The summation must then be performed over the $\Omega = 1$ states. According to the *ab initio* calculations, these states are linear combinations of those defined in the separated-atom representation. According to reference [10], the actual states are :

$$\begin{aligned} \langle\langle 1'_u \rangle\rangle &= 0.90 |1'_u\rangle - 0.44 |1''_u\rangle \\ \langle\langle 1''_u \rangle\rangle &= 0.90 |1''_u\rangle + 0.44 |1'_u\rangle \\ \langle\langle 1'_g \rangle\rangle &= 0.84 |1'_g\rangle + 0.54 |1''_g\rangle \\ \langle\langle 1''_g \rangle\rangle &= 0.84 |1''_g\rangle - 0.54 |1'_g\rangle, \end{aligned}$$

in which the right hand side refers to states of the separated-atom basis, the mixing coefficients being given for an internuclear distance $R = 10 \text{ \AA}$.

In order to evaluate all the different contributions to the effective parameters, the sum $S(v') = \sum \frac{\langle v|v'\rangle^2}{\Delta E_{vv'}^{J'}}$ has to be calculated for each Ω state. This requires the knowledge of the entire potential curves. Unfortunately, the perturbing Ω states are

poorly known experimentally. The best available data are from the *ab initio* calculations [10a, b], which are valid for $R > 7 \text{ \AA}$ (see Fig. 5), so that accurate calculation of the $S(v')$ values cannot be performed. However, as we are dealing with high vibrational B state levels, practically all the contribution to the overlap integral $\langle v|v' \rangle$ comes from the outer limb of the potential curve. Moreover the *ab initio* long range potential curves are good estimates of the actual curves as can be seen by comparison with experimental long range parameters [3, 11] or with long range interactions [12]. Then a good estimate of the $S(v')$ value can be made with the completion of the long-range potential curve by an approximate Morse potential using estimated potential depth D_e and equilibrium internuclear distance R_e for the experimentally unknown or poorly known perturbing states.

For example for the « $1'_g$ » state we tried values in the range $400 < D_e < 900 \text{ cm}^{-1}$ and $3.5 < R_e < 3.8 \text{ \AA}$ and the most satisfying solutions with respect to our experimental results (see Sect. 3.3.3 of this paper) were for the $700\text{-}900 \text{ cm}^{-1}$ D_e range (see Ref. [9] p. 289). This is in agreement with the determinations of reference [13] which gives for a weakly bound state converging to the same dissociation limit $D_e = 864 \text{ cm}^{-1}$ and $R_e = 3.645 \text{ \AA}$.

Other potential curves for calculating $S(v')$ have been used in the $200 < D_e < 400 \text{ cm}^{-1}$ and $4 < R_e < 5 \text{ \AA}$ range where the $2u$ state was estimated to be [14-16].

With the above assumptions, the $S(v')$ sum can be evaluated numerically. The results show three interesting features :

i) For non-resonant perturbing levels, the main contributions to $S(v')$ come from the perturbing vibrational levels having an outer turning point near $r_+(v')$, $r_+(v')$ being the outer turning point of the B state v' level : this corresponds to the Franck-Condon principle.

ii) The position of these main perturbing levels depends on the choice of D_e and R_e , but the resulting sum $S(v')$ remains constant in a first approximation, so that a rough D_e and R_e estimate is sufficient for our purpose.

iii) For resonant perturbing levels, which will be studied later, the only significant contribution comes from the « $1'_g$ » state.

Finally the $S(v')$ determination can be simplified if we calculate the quantity :

$$S'(v') = \Delta E_+(v') S(v'), \quad (4)$$

in which $\Delta E_+(v')$ is defined as :

$$\Delta E_+(v') = \frac{C_5(B) - C_5(\Omega)}{r_+^5(v')} + \frac{C_6(B) - C_6(\Omega)}{r_+^6(v')}$$

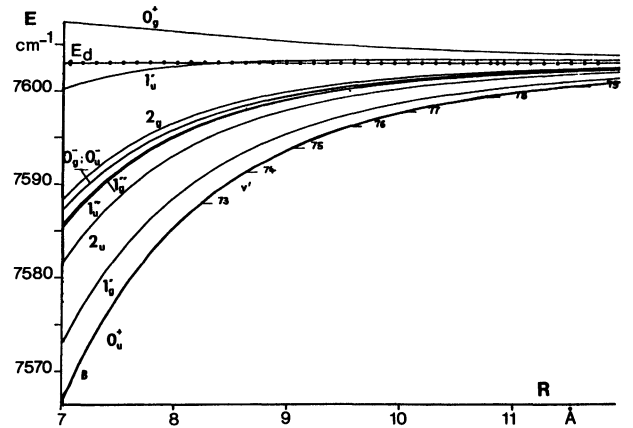


Fig. 5. — *Ab initio* potential curves of the 10 electronic states near the iodine $^2P_{1/2} + ^2P_{3/2}$ dissociation limit (Ref. [10]). E_d denotes the dissociation limit. The origin of the energy scale is taken at the first dissociation limit $^2P_{3/2} + ^2P_{3/2}$. The quotation marks for the « $1'_g$ », « $1'_u$ », « $1''_g$ » and « $1''_u$ » states have been omitted.

$\Delta E_+(v')$ represents the energy separation between the B state and the perturbing states evaluated at the outer turning point $r_+(v')$; C_5 and C_6 are the long-range parameters of the potential curve for each state [10]. The $S'(v')$ value has been found to change only little for v' varying from 70 to 82, so that all the $S(v')$ values can be deduced from one $S'(v')$ calculation by the relation (4).

All the contributions to the effective parameters C' , δ' , d' and eQq' given by the relation (2) can then be calculated for each v' B state level. The results are summarized in tables I to IV, together with the experimental results. The predicted values are in good agreement with the measurements, confirming the validity of our approximations and of the separated atom basis for long-range hyperfine structure calculations.

The examination of table I shows that 6 states are contributing to the eQq' variation, with a dominating positive effect of all the $\Omega = 1$ states with respect to $\Omega = 0$ states, and this variation is magnetic dipolar in origin. The effect of the $\Omega = 0$ and 1 states is not clear in the case of the d' and δ' parameters, since cancellation effects between the various contributions arise, so that a predominant perturbing state is difficult to distinguish. So the sign and value of d' and δ' determined from very high resolution measurements for $v' = 58$ [17] and $v' = 62$ [7] cannot be due to an interaction with the 0_g^- state as suggested by the authors of references [17] and [7]. Besides, that interpretation can be checked with our model, which is still surprisingly valid for these levels (they correspond to $r_+ = 5.50$ and 5.95 \AA) and gives the correct sign and order of magnitude of the hyperfine B 0_u^+ parameters in that range [9].

The C' dependence on v' is remarkably well described by the theoretical predictions. From $v' = 71$ to $v' = 82$, the C' value increases by about one order of magnitude. As a consequence the spin-

Table I. — Contribution of the various electronic (1/2 – 3/2) states to the effective parameter eQq' value in the second order perturbation theory (relation (2)), and the corresponding experimental determinations. The theoretical value is the sum of all the contributions plus the first order term eQq'_0 with $eQq'_0 = -573$ MHz. The $\Omega = 1$ states give two different contributions (relations (3)). The first line corresponds to eQq'_{11} and the second to $eQq'_{12} + eQq'_{21}$. For the $1'_u$ and $1'_g$ states, the latter contribution is negligible and is not given in the table. The $\Omega = 2$ states give a negligible contribution. All values are in MHz.

v'	r^+ (Å)	0_g^-	0_u^+	0_u^-	$1''_g$	$1'_g$	$1'_u$	$1''_u$	$eq'Q_{th}$	$eq'Q_{exp}$
71	7.607	– 3.64	0	– 2.18	1.24 1.82	6.68	4.50	2.14 3.14	– 559	– 555 ± 2
72	7.891	– 4.41	0	– 2.64	1.51 2.22	8.06	5.47	2.59 3.80	– 555	– 552 ± 2
73	8.209	– 5.43	0	– 3.25	1.85 2.72	9.88	6.72	3.17 4.66	– 552	– 548 ± 4
74	8.565	– 6.78	0	– 4.46	2.31 3.38	12.3	8.40	3.95 5.80	– 549	– 543 ± 2
75	8.969	– 8.63	0	– 5.17	2.93 4.30	15.6	10.7	5.01 7.36	– 540	– 537 ± 5
76	9.431	– 11.2	0	– 6.71	3.80 5.58	20.3	13.9	6.48 9.52	– 531	
77	9.969	– 14.9	0	– 8.93	5.03 7.39	26.9	18.4	8.58 12.6	– 518	
78	10.59	– 20.5	0	– 12.3	6.90 10.1	37.0	25.3	11.8 17.3	– 497	
79	11.35	– 29.2	0	– 17.4	9.77 14.4	52.1	35.9	16.6 24.4	– 466	– 460 ± 10
80	12.28	– 43.3	0	– 25.9	14.5 21.3	76.6	53.4	24.6 36.1	– 416	– 430 ± 12
81	13.46	– 67.7	0	– 40.6	22.5 33.1	116.	83.8	38.3 56.3	– 331	– 380 ± 10
82	14.83	– 113.	0	– 67.7	37.4 54.9	189.	141.	63.5 93.3	– 175	– 290 ± 20

Table II. — Contribution of the 1_u states to the C' value (relations (2)), in which C'_D is neglected (Ref. [8a]), and comparison to the experimental determinations C'_{exp} . All values are in MHz.

v'	r_+ (Å)	$1'_u$	$1''_u$	C'_{th}	C'_{exp}
71	7.607	1.38	0.88	2.20	2.16 ± 0.07
72	7.891	1.55	0.92	2.47	2.36 ± 0.08
73	8.209	1.76	1.04	2.79	2.83 ± 0.10
74	8.565	2.01	1.18	3.18	3.16 ± 0.15
75	8.969	2.32	1.36	3.67	3.65 ± 0.18
76	9.431	2.71	1.58	4.29	4.45 ± 0.14
77	9.969	3.21	1.87	5.07	
78	10.59	3.88	2.25	6.13	
79	11.35	4.78	2.76	7.55	7.6 ± 0.5
80	12.28	6.05	3.48	9.53	10.0 ± 0.5
81	13.46	7.90	4.51	12.4	13 ± 1
82	14.83	10.7	6.06	16.8	16 ± 1

rotation interaction (equal to $C'I'J'$) becomes predominant for large J' values, and the hyperfine structure width is given almost entirely by this term. On the other hand, for low J' values, the J' — diagonal scalar spin-spin interaction dominates the h.f.s., so that the molecular nuclear spin I' becomes a good quantum number near the dissociation limit.

3.2 SUPERHYPERFINE STRUCTURES. — It is well known that the rotational constant B'_v decreases with increasing vibrational quantum number v' and vanishes at the dissociation limit. This means that for small rotational separations such as in band heads, it may happen that rotational structure becomes weaker than the hyperfine structure of each level. For example in the B state, we have for $v' = 75$ a B'_v value of 154 MHz [3], while the h.f.s. is of the order of 2 GHz. The interpretation of the structure can be made with the same Hamiltonian as in the preceding section, but the related interaction matrix has to be developed on the full space spanned by all the neighbouring rotational states.

Table III. — Contribution of the various electronic ($1/2 - 3/2$) states to the δ' value (relations (2)) and the corresponding experimental results, in MHz.

v'	r_+ (Å)	0_g^-	0_u^+	0_u^-	$1_g''$	$1_g'$	$1_u'$	$1_u''$	δ'_{th}	δ'_{exp}
71	7.607	3.64	0	- 2.18	1.24	6.68	- 4.50	- 2.14	2.74	3.56 ± 0.04
72	7.891	4.41	0	- 2.64	1.51	8.06	- 5.47	- 2.59	3.29	3.72 ± 0.04
73	8.209	5.43	0	- 3.25	1.85	9.88	- 6.72	- 3.17	4.02	4.45 ± 0.08
74	8.565	6.78	0	- 4.06	2.31	12.3	- 8.40	- 3.95	4.98	4.92 ± 0.10
75	8.969	8.63	0	- 5.17	2.93	15.6	- 10.7	- 5.01	6.34	5.68 ± 0.08
76	9.431	11.2	0	- 6.71	3.80	20.3	- 13.9	- 6.48	8.22	
77	9.969	14.9	0	- 8.93	5.03	26.9	- 18.4	- 8.58	10.9	
78	10.59	20.5	0	- 12.3	6.90	37.0	- 25.3	- 11.8	15.0	
79	11.35	29.2	0	- 17.4	9.77	52.1	- 35.9	- 16.6	21.2	23 ± 1
80	12.28	43.3	0	- 25.9	14.5	76.6	- 53.4	- 24.6	30.5	38 ± 2
81	13.46	67.7	0	- 40.6	22.5	117.	- 83.8	- 38.3	44.1	65 ± 4
82	14.83	113.	0	- 67.7	37.4	189.	- 141.	- 63.5	67.9	98 ± 10

Table IV. — Contribution of the various electronic ($1/2 - 3/2$) states to the d' value (relations (2)), with $d'_D = 0$ (Ref. [8a]), and the experimental determinations, in MHz.

v'	r_+ (Å)	0_g^-	0_u^+	0_u^-	$1_g''$	$1_g'$	$1_u'$	$1_u''$	d'_{th}	d'_{exp}
71	7.607	- 3.64	0	2.18	0.62	3.34	- 2.25	- 1.07	- 0.82	$- 0.90 \pm 0.10$
72	7.891	- 4.41	0	2.64	0.76	4.03	- 2.74	- 1.30	- 1.02	$- 1.1 \pm 0.08$
73	8.209	- 5.43	0	3.25	0.93	4.94	- 3.36	- 1.59	- 1.26	$- 1.5 \pm 0.2$
74	8.565	- 6.78	0	4.06	1.16	6.15	- 4.20	- 1.98	- 1.59	$- 1.7 \pm 0.2$
75	8.969	- 8.63	0	5.17	1.47	7.82	- 5.34	- 2.51	- 2.02	$- 2.7 \pm 0.2$
76	9.431	- 11.2	0	6.71	1.90	10.2	- 6.95	- 3.24	- 2.59	
77	9.969	- 14.9	0	8.93	2.52	13.5	- 9.20	- 4.29	- 3.44	
78	10.59	- 20.5	0	12.3	3.45	18.5	- 12.7	- 5.90	- 4.85	
79	11.35	- 29.2	0	17.4	4.89	26.1	- 18.0	- 8.52	- 7.13	$- 10.5 \pm 1.5$
80	12.28	- 43.3	0	25.9	7.25	38.1	- 26.7	- 12.3	- 10.9	$- 17 \pm 5$
81	13.46	- 67.7	0	40.6	11.3	58.3	- 41.9	- 19.2	- 18.6	$- 31 \pm 7$
82	14.83	- 113.	0	67.7	18.7	94.6	- 70.3	- 31.8	- 34.1	$- 50 \pm 8$

The resulting h.f.s., called superhyperfine structures [6a, b] have been observed in several band heads in this work. Spreading and rearrangement of the h.f.s. patterns are observed through the influence of the non-diagonal quadrupolar and tensorial spin-spin terms. The results are visualized in figure 6. The mutual $J' = 0$ and $J' = 2$ perturbation modifies the h.f.s. For clarity, the h.f.s. before (dashed lines) and after (full lines) introducing the non-diagonal matrix elements are given only for the three hyperfine sublevels of the $J' = 0$ level (Fig. 6). As a consequence the centre of gravity of the $J' = 0$ h.f.s. pattern is displaced, i.e. is lowered in the energy scale. Figure 7 gives the predicted magnitude of this displacement. Our absolute frequency measurements with the lambda-meter compared with the position of the unshifted lines calculated from the constants of reference [18] agree with these predictions within our experimental accuracy.

This study clearly shows that the hyperfine interactions must be taken into account for high precision measurements in the long-range rovibrational analysis of the I_2 B state [3, 18]. Indeed near the dissociation limit the only observable levels are the first J' values, and the observed line positions have to be corrected for the hyperfine shifts. Nevertheless this correction is small up to $v' = 82$ since the shift remains lower than 0.010 cm^{-1} .

3.3 THE u-g PERTURBATION. — In the preceding sections the study of the $v' = 77$ and 78 vibrational levels has been left out. For these levels the observed h.f.s. patterns are completely different from those that can be generated with any set of effective parameters in the second-order approximation. Obviously the weak perturbation treatment becomes inadequate and a strong perturbation approach must be taken. But before dealing with these levels, we

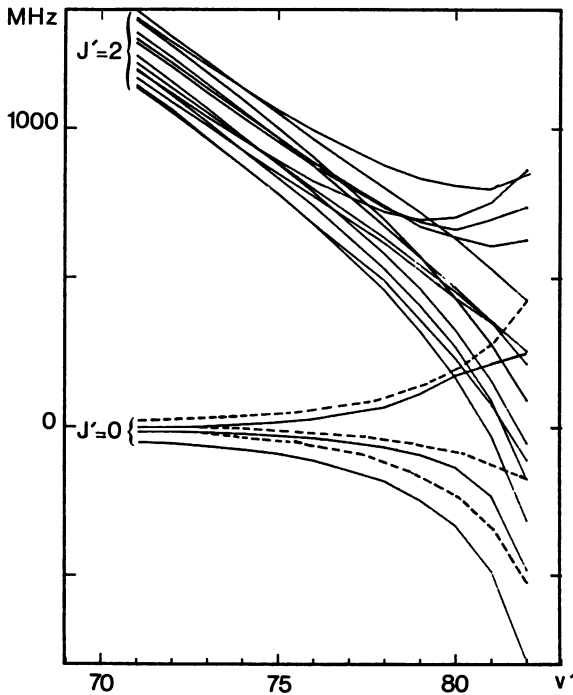


Fig. 6. — The hyperfine perturbation of the $J' = 0$ hyperfine structure (h.f.s.) by the $J' = 2$ level, in several band heads (superhyperfine structure). Dashed lines and full lines are respectively the $J' = 0$ h.f.s. neglecting and introducing the $J' = 2$ perturbation.

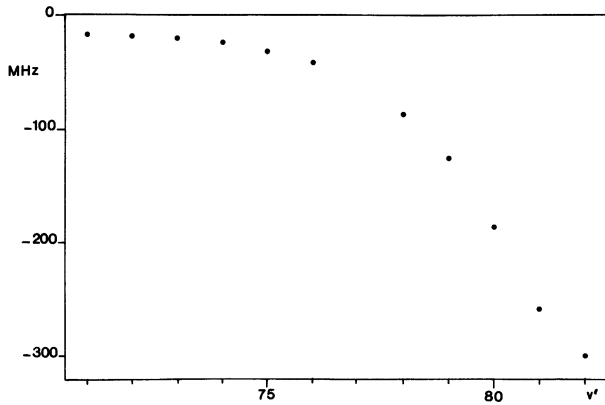


Fig. 7. — Predicted displacement of the centre of gravity of the $J' = 0$ h.f.s. pattern due to the $J' = 2$ hyperfine perturbation.

have to return to the case of the neighbouring $v' = 76$ level in which h.f.s. anomalies have already been mentioned in section 3.1, which presumably represents a transition between weak and strong perturbations.

3.3.1 Anomalies in the $v' = 76$ level. — If the second-order perturbation treatment is still valid in $v' = 76$, the results shown in figures 3 and 4 exhibit a strong J' dependence of all effective parameters except C' . In more detail the d' and δ' variations with the quantity $J'(J' + 1)$ are given in the figures 8 and 9. Clearly, these variations are linear with

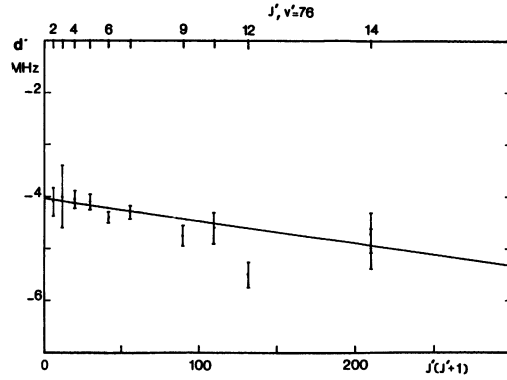


Fig. 8. — J' -dependence of the tensorial spin-spin effective parameter d' in the $v' = 76$ level. The error bars represent \pm two standard deviations in the fits.

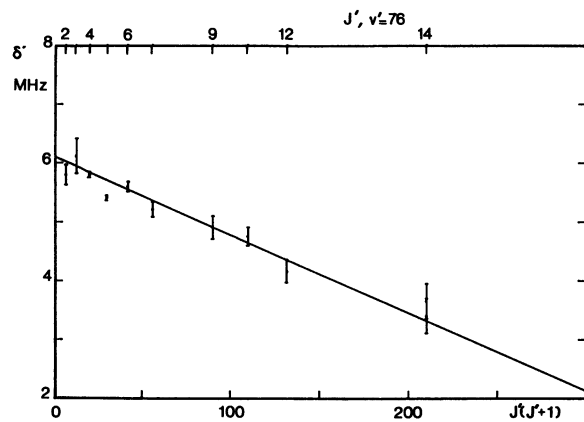


Fig. 9. — J' -dependence of the scalar spin-spin effective parameter δ' in the $v' = 76$ level.

$J'(J' + 1)$, with a negative slope. Although the eQq determination is poorer, the same conclusions can be said about the $eQq' J'$ dependence.

This behaviour indicates that a rotational crossing between the B state ($v' = 76, J'$) and a perturbing Ω^* state vJ level occurs at some J' . Several facts lead us to the identification of the Ω^* perturbing state. The first is the absence of any C' perturbation: the $1_u'$ and $1_u''$ states, which are the only states contributing to C' , cannot be the Ω^* state. The second fact comes from the theoretical interpretation of the d', δ' and $eQq' J'$ dependence.

Returning to the expressions (2) of the effective parameters, we write the energy separation as:

$$\Delta E_{vv'}^{J'} \simeq \Delta E_{vv'} + \Delta B J'(J' + 1)$$

with

$$\Delta B = B_v(\Omega^*) - B_{v'}(0_u^+)$$

and

$$\Delta E_{vv'} = E_{\Omega^*, v', J' = 0}^* - E_{0_u^+, v, J' = 0}$$

(the $\Omega^*, J' = 0$ level being real or not).

If only one Ω^* vibrational ν level perturbs the B state level, we can write :

$$\delta' = \delta'_{11}(\Omega^*) \frac{\Delta E_{\nu\nu'}}{\Delta E_{\nu\nu'} + \Delta B J'(J'+1)} + \sum_{\Omega \neq \Omega^*} \delta'_{11}(\Omega).$$

As $\Delta B J'(J'+1) \ll \Delta E_{\nu\nu'}$, we have to a good approximation :

$$\delta' = -\delta'_{11}(\Omega^*) \frac{\Delta B}{\Delta E_{\nu\nu'}} J'(J'+1) + \sum_{\Omega} \delta'_{11}(\Omega).$$

Similarly, we have for the other parameters :

$$d' = -d'_{11}(\Omega^*) \frac{\Delta B}{\Delta E_{\nu\nu'}} J'(J'+1) + \sum_{\Omega} d'_{11}(\Omega)$$

$$eQq' = -eQq'(\Omega^*)$$

$$\times \frac{\Delta B}{\Delta E_{\nu\nu'}} J'(J'+1) + \sum_{\Omega} eQq'(\Omega).$$

The above relations ensure a linear variation of the parameters with J' ($J'+1$). As the observed slopes of these variations are all negative we are led to the conclusion that

$$\delta'_{11}(\Omega^*), d'_{11}(\Omega^*) \text{ and } eQq'(\Omega^*)$$

must all be of the same sign. An examination of tables I, III and IV clearly shows that only the « $1'_g$ » and « $1''_g$ » states fulfill this condition. Moreover, the slope ratio δ'/d' in figures 8 and 9 is approximately equal to 2, which is its theoretical value for the $\Omega = 1$ states.

From the *ab initio* calculations (10), the ΔB value can be estimated for the « $1'_g$ » and « $1''_g$ » states. For the « $1'_g$ » state we have $\Delta B \approx 15$ MHz and for the « $1''_g$ » state, $\Delta B \approx 350$ MHz. Obviously, the latter value is far too large to give near-resonant conditions over several J' values, the B state $B'_{v'=76}$ value being of the order of 140 MHz. As a conclusion, the Ω^* state is the « $1'_g$ » state, and following studies will confirm this statement.

3.3.2 Hyperfine structure in the $v' = 77$ and 78 levels.

— The definitive evidence of the « $1'_g$ » - 0_u^+ perturbation is obtained after the fits using the direct diagonalization of the complete interaction matrix. The selection rules established in part I show that for each F' value, 5 rotational levels have to be included ($\Delta J = 0, \pm 1, \pm 2$) and for each rotational level, three nuclear spin I values are possible. Moreover, we must take into account the two c_+ and c_- substates of a $\Omega = 1$ state, so that the resulting matrices have a dimension of 45×45 . The derivation

of all the matrix elements involves the calculation of :

i) The eQq' , C' , d' and δ' parameters with the contribution given by all the interacting states reported in tables I to IV, « $1'_g$ » excepted ;

ii) The h.f.s. of the « $1'_g$ » state, which to first order is electric quadrupolar and magnetic dipolar, and can be calculated *ab initio* in the separated-atom basis set ;

iii) The non-diagonal matrix elements between the 0_u^+ - « $1'_g$ » states, given in part I ;

iv) The weighted overlap sum $S(v')$.

The rotational constants B'_{77} and B'_{78} are taken from references [3] or [18]. From what we know about the « $1'_g$ » state, it is reasonable to assume that the B 0_u^+ and « $1'_g$ » vibrational spacings are comparable in the perturbation region. If we call ν the « $1'_g$ » vibrational level perturbing the $v' = 76$ level of the B state, the main perturbers of $v' = 77$ and 78 are then $\nu + 1$ and $\nu + 2$ respectively. The only floating parameters in the fits are then the energy separations :

$$\Delta E_{v+1,77} = E'_{1g}(v+1, J=0) - E_{0u^+}(v'=77, J'=0)$$

$$\Delta E_{v+2,78} = E'_{1g}(v+2, J=0) - E_{0u^+}(v'=78, J'=0)$$

and the rotational constants B_{v+1} and B_{v+2} of the « $1'_g$ » state.

3.3.2.1 The $v' = 77$ level analysis. — The h.f.s. analysis for various J' values has been possible with the observation of five well-resolved rotational lines : P (28), R (27), R (19), R (11) and R (0). The obtained parameters are consistent with :

$$B_{v+1} = 120 \pm 5 \text{ MHz}$$

and

$$\Delta E_{v+1,77} = 4.5 \pm 0.5 \text{ GHz.}$$

The perturbation by the « $1'_g$ » state is essentially magnetic dipolar. A given B state ($v' = 77, J'$) level can then be perturbed by three different « $1'_g$ » state levels :

$$(c_-, v+1, J=J'+1), (c_+, v+1, J=J')$$

and $(c_-, v+1, J=J'-1)$. The above results allow the study of the $1'_g - 0_u^+$ crossing with J' for the three interacting « $1'_g$ » levels. Figure 10 represents the energy separation between the two states as a function of J' , for each « $1'_g$ » sub-level. This figure clearly shows that the h.f.s. depends strongly on the c_+ or c_- character of the « $1'_g$ » perturbing state.

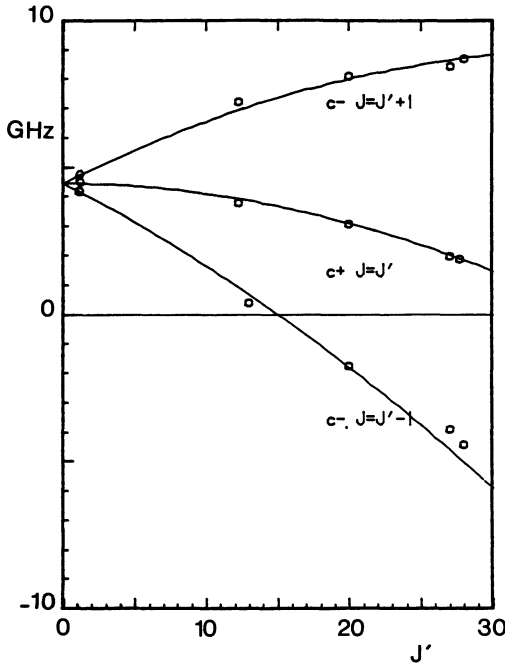


Fig. 10. — Predicted energy separations in GHz $E(1'_g, v+1, J) - E(B 0_u^+, v=77, J')$ as a function of J' , for the three perturbing $1'_g$ sublevels. The full lines are calculated from the parameters determined in the fits (see Sect. 3.3.2.1). The quasi-resonance of the c_+ , $J=J'+1$ sublevel occurs near $J'=36$ (not shown in the figure).

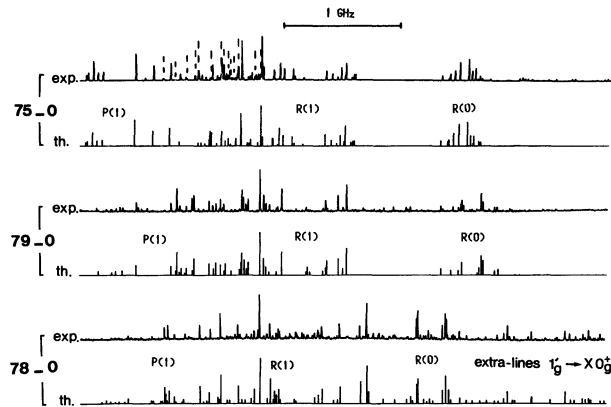


Fig. 11. — The 75-0, 79-0 and 78-0 band head spectrum. The first two cases are interpreted with the second-order perturbation theory, while the third case corresponds to the direct diagonalization of the full interaction matrix. Evidence of the u-g perturbation is given by the observation of the $1'_g \rightarrow X 0_g^+$ forbidden transition near the 78-0 band head. The dashed lines in the 75-0 band head spectrum belong to other bands.

It can be noted that two quasi-resonant interactions must occur at the $J'=15$ and 36 levels with respectively c_- and c_+ substates, but their experimental study has not been possible, since the relevant lines are almost totally overlapped by other features.

3.3.2.2 The 78-0 band head: the forbidden $1'_g - X 0_g^+$ transition. — Figure 11 gives three different band head spectra, which are from the 75-0, 79-0 and 78-0 bands. The 75-0 and 79-0 experimental spectra can be interpreted in the second-order approximation. By comparison with these two cases, the hyperfine spectrum of the 78-0 band head is completely different. The direct diagonalization of the full interaction matrix has been performed, all the hyperfine parameters being fixed at their *ab initio* predicted values in the separated-atom approach calculated as explained previously (see also Ref. [19]):

$$B 0_u^+ \text{ parameters : } eQq' = -534 \text{ MHz}$$

$$C' = 6.1 \text{ MHz,}$$

$$\ll 1'_g \gg \text{ parameters : } eQq = -224 \text{ MHz}$$

$$C = \frac{3886}{J(J+1)} \text{ MHz}$$

and

$$\langle 0_u^+ | \bar{V}^1 | \ll 1'_g \gg \rangle = -2340 \text{ MHz}$$

$$\langle 0_u^+ | \bar{V}^2 | \ll 1'_g \gg \rangle = -446 \text{ MHz.}$$

The fit gives for the floating parameters :

$$\Delta E_{v+2,78} = 1800 \pm 300 \text{ MHz}$$

$$B_{v+2} = 100 \pm 10 \text{ MHz.}$$

Then the theoretical spectra allow us to identify the hyperfine components. This gives the first direct evidence of a u-g perturbation. In particular the assignment of a group of lines to the forbidden $\ll 1'_g \gg - X 0_g^+$ transition, issued from the $J=1 \ll 1'_g \gg$ sublevels, is the first example of extra-lines occurring because of hyperfine mixing. These extra lines confirm the mixing of nuclear spins of odd and even parity. As a consequence, the ortho and para character of the related levels is not defined in the presence of strong hyperfine interactions, in agreement with the theoretical predictions.

3.3.3 Consequences of our determination. — The interpretation of the u-g perturbation observed in $B 0_u^+ v'=76, 77$ and 78 levels has given the following data for the $\ll 1'_g \gg$ state :

$$B_v = 155 \pm 10 \text{ MHz}$$

$$B_{v+1} = 120 \pm 5 \text{ MHz}$$

$$B_{v+2} = 100 \pm 10 \text{ MHz}$$

$$\Delta E_{v+1,77} = 4.5 \pm 0.5 \text{ GHz}$$

$$\Delta E_{v+2,78} = 1.8 \pm 0.3 \text{ GHz}$$

These data allowed us to construct a $\ll 1'_g \gg$ potential curve as indicated in 3.1.2 with a better precision.

We have found [9] that D_e has to be large at the limit of our pre-estimation : $\sim 900 \text{ cm}^{-1}$. But our data are insufficient to define R_e . When we use $R_e = 3.64 \text{ \AA}$ as in reference [13] we find $v = 46$ and taking account of our various approximations the « $1'_g$ » parameters are recalculated correctly (see the Ref. [9]).

Moreover some intriguing previous observations of King *et al.* [20] can be explained now. From Optical-Optical double resonance, the first step being high vibrational levels of $B 0_u^+$, these authors succeeded in exciting 5 electronic states $\alpha, \beta, \gamma, \delta, \epsilon$ of the first group of 6 ionic states ($0_g^+, 1_g, 2_g, 0_u^+, 1_u, 2_u$) [1].

From a pure $B 0_u^+$ state only gerade levels can be excited, and indeed the ϵ state has been identified as $E 0_g^+$ [21, 22], the β state as 1_g [22] and the α state as $D' 2_g$ [15]. Only a $1_g - D' 2_g$ mixing can explain the $B 0_u^+ \rightarrow D' 2_g$ transition, since we have shown that the $B 0_u^+ - 1_u'$ or $1_u''$ mixings are negligible.

Now the γ and δ states are ungerade states and can be excited from $B 0_u^+$ rotational levels mixed with « $1'_g$ » through hyperfine perturbations. It has to be noted that relatively intense excitations have been observed [20] in the $B 0_u^+$ ($v' = 77, 78$) range where we have found strong u-g mixing. Then γ is probably the 1_u state, since no Q lines were observed for the $B 0_u^+ (1'_g) \rightarrow \gamma$ transition. The δ state would then be 0_u^+ or 2_u ; as the $D (0_u^+)$ state has been observed at low v' [23] the δ state is almost certainly 2_u . Consequently the study of any ionic state of either gerade or ungerade symmetry is made possible in Optical-Optical double resonance *via* the u-g perturbed $B 0_u^+$ levels.

4. Conclusion.

Using a supersonic molecular beam together with powerful numerical data processing enabled us to carry out a systematic survey of the hyperfine structure of the iodine $B 0_u^+$ state. Extending the previous works to the observation of high vibrational levels, we have shown that numerous features can be explained from the second-order theory of Vigué, Broyer, Lehmann [2]. But we have found vibrational levels with totally unusual hyperfine patterns where only a direct perturbation treatment allowed us to calculate the structure. So we have clearly shown that u-g mixing with a $1g$ state appears for different rotational levels of the $B 0_u^+$ state. The hyperfine patterns can be recalculated in a separated atom basis which allows a good physical insight in the experimental observations. However, the hyperfine analysis in iodine is not closed so far. For example the « $1'_g$ » state is only indirectly known through its perturbation of the B state, and a complete description of the B state hyperfine structure needs an accurate knowledge of the « $1'_g$ » state. On the other hand, such hyperfine behaviour near a dissociation limit is not restricted to the iodine molecule. Similar effects are likely to be met in any homonuclear diatomic molecule having hyperfine structure large enough to become comparable to the other energy separations near the dissociation limit, as has for example been recently observed in the Cs_2 molecule [24].

Acknowledgments.

M. Saute and M. Aubert-Frécon are greatly acknowledged for communicating us unpublished results on their separated-atom analysis of iodine states.

References

- [1] MULLIKEN, R. S., *J. Chem. Phys.* **55** (1971) 288.
- [2] a) BROYER, M., VIGUE, J. and LEHMANN, J. C., *J. Physique* **39** (1978) 591 ;
b) VIGUE, J., BROYER, M. and LEHMANN, J. C., *Phys. Rev. Lett.* **42** (1979) 883 ;
c) VIGUE, J., BROYER, M. and LEHMANN, J. C., *J. Physique* **42** (1981) 937.
- [3] GERSTENKORN, S., LUC, P. and AMIOT, C., *J. Physique* **46** (1985) 355.
- [4] CHURASSY, S. GRENET, G., GAILLARD, M. L. and BACIS, R., *Opt. Commun.* **30** (1979) 41.
- [5] CACHENAUT, J., MAN, C., CEREZ, P., BRILLET, A., STOECKEL, F., JOURDAN, A. and HARTMANN, F., *Rev. Phys. Appl.* **14** (1979) 685.
- [6] a) HARTEY, W. G., *Phys. Rev. A* **24** (1981) 192 ;
b) BORDE, J. and BORDE, Ch. J., *Chem. Phys.* **71** (1982) 417.
- [7] BORDE, C., CAMY, G., DECOMPS, B. DESCOUBES, J. P. and VIGUE, J., *J. Physique* **42** (1981) 1393.
- [8] a) BROYER, M., Thèse, Paris VI (1977) ;
b) VIGUE, J., Thèse, Paris VI (1978).
- [9] PIQUE, J. P., Thèse, Grenoble (1984).
- [10] a) SAUTE, M. and AUBERT-FRECON, M., *Chem. Phys. Lett.* **86** (1982) 59 ;
b) SAUTE, M. and AUBERT-FRECON, M., *J. Chem. Phys.* **77** (1982) 5639 ;
c) SAUTE, M. and AUBERT-FRECON, M., Private communications.
- [11] BACIS, R., CERNY, D., MARTIN, F., *J. Mol. Spectrosc.* **118** (1986) 434.
- [12] MARTIN, F., CHURASSY, S., BACIS, R., FIELD, R. W. and VERGES, J., *J. Chem. Phys.* **79** (1983) 3725.
- [13] ISHIWATA, T., OHTOSHI, H., SAKAKI, M., TANAKA, I., *J. Chem. Phys.* **80** (1984) 1411.
- [14] GUY, A. L., VISWANATHAN, K. S., SUR, A. and TELLINGHUISEN, J., *Chem. Phys. Lett.* **73** (1980) 582.
- [15] KOFFEND, J. B., SIBAI, A. M. and BACIS, R., *J. Physique* **43** (1982) 1639.

- [16] TELLINGHUISEN, J., *J. Phys. Chem.* **87** (1983) 5136.
- [17] FOTH, H. J. and SPIEWECK, F., *Chem. Phys. Lett.* **65** (1979) 347.
- [18] GERSTENKORN, S. and LUC, P., *J. Physique* **46** (1985) 867.
- [19] PIQUE, J. P., HARTMANN, F., BACIS, R., CHURASSY, S. and KOFFEND, J. B., *Phys. Rev. Lett.* **52** (1984) 267.
- [20] a) DANYLUK, M. D. and KING, G. W., *Chem. Phys.* **22** (1977) 59 ;
b) KING, G. W., LITTLEWOOD, I. M. and ROBINS, J. R., *Chem. Phys.* **56** (1981) 145.
- [21] WIELAND, K., TELLINGHUISEN, J. B. and NOBS, A., *J. Mol. Spectros.* **41** (1972) 69.
- [22] CHEVALEYRE, J., PERROT, J. P., CHASTANG, J. M., VALIGNAT, S. and BROYER, M., *Chem. Phys.* **67** (1982) 59.
- [23] VISWANATHAN, K. S. and TELLINGHUISEN, J., *J. Mol. Spectros.* **101** (1983) 285.
- [24] a) WEICKENMEIER, W., DIEMER, U., WAHL, M., RAAB, M., DEMTRÖDER, W. and MÜLLER, W., *J. Chem. Phys.* **82** (1985) 5354 ;
b) WEICKENMEIER, H., DIEMER, U., DEMTRÖDER, W. and BROYER, M., *Chem. Phys. Lett.* **124** (1986) 470.
-